Title: Transcriptional Atlas of Ileal-Anal Pouch Immune Cells from Ulcerative Colitis Patients

Authors: Joseph C. Devlin[1,2,6,*], Jordan Axelrad[3*], Ashley M. Hine[1,3*], Shannon Chang[3], Suparna Sarkar[4], Jian-Da Lin[1,8], Kelly V. Ruggles[5,6], David Hudesman[3], Ken Cadwell[1,3,8], P'ng Loke[1,8]

Affiliations:

[1]Department of Microbiology, New York University Grossman School of Medicine, New York, NY 10016, USA.

[2]Sackler Institute of Graduate Biomedical Sciences, New York University Grossman School of Medicine, New York, NY 10016, USA.

[3]Division of Gastroenterology and Hepatology, Department of Medicine, New York University Grossman School of Medicine, New York, NY 10016, USA.

[4]Department of Pathology, New York University Grossman School of Medicine, New York, NY 10016, USA

[5]Division of Translational Medicine, Department of Medicine, New York University Grossman School of Medicine, New York, NY 10016, USA.

[6]Institute of Systems Genetics, New York University Grossman School of Medicine, New York, NY 10016, USA.

[7]Laboratory of Parasitic Diseases, National Institute of Allergy and Infectious Diseases, National Institutes of Health, Bethesda, MD 20892, USA.

[8]Skirball Institute of Biomedical Medicine, New York University Grossman School of Medicine, New York, NY 10016, USA.

*These authors contributed equally

Correspondence to:

Png.Loke@nih.gov

Ken.Cadwell@med.nyu.edu

Jordan.Axelrad@nyulangone.org

ABSTRACT

How the human intestinal immune system is distinctly organized to respond to inflammation is still poorly understood. Here, we used single-cell RNA-sequencing to examine lamina propria CD45+ hematopoietic cells from patients with inflammatory bowel disease that have undergone ileal pouch-anal anastomosis, or the colon mucosa of ulcerative colitis patients. We identified a population of *IL1B*+ antimicrobial macrophages and *FOXP3*/+*BATF*+ T cells that are associated and expanded in inflamed tissues, which we further validated in other scRNA-seq datasets from IBD patients. CD8+ T cells were unexpectedly more abundant in the pouch than colon. Cell type specific markers obtained from single-cell RNA-sequencing was used to infer representation from bulk RNA sequencing datasets, which further implicated antimicrobial macrophages expressing *IL1B* with *S100A8/A9* calprotectin as being associated with inflammation, as well as *Bacteroides* and *Escherichia* bacterial species. Finally, we find that non-responsiveness to anti-integrin biologic therapies in UC patients is associated with the signature of this antimicrobial macrophage population in a subset of patients. This study identified conserved and distinct features of intestinal inflammation between parts of the small and large intestine undergoing similar inflammation conditions.

INTRODUCTION

The intestinal immune system is organized distinctly between anatomically defined segments that have different physiological functions. Whereas immune cells in the small intestine protect the epithelium from infection to enable nutrient absorption while maintaining tolerance to dietary antigens, the large intestine must maintain a détente with the large number of commensal bacteria without triggering overt inflammation. This fine balance breaks down in the context of inflammatory bowel diseases (IBD) such as ulcerative colitis (UC) and Crohn's disease (CD), whereby inflammatory damage to the epithelium results in mucosal ulceration causing diarrhea, bleeding, and abdominal pain. Restorative proctocolectomy with ileal pouch-anal anastomosis (IPAA) is a common surgical procedure in UC patients with medically refractory disease[1]. The ileal pouch reservoir, or J-pouch, is a novel organ created from small intestine formed into a J-shaped pouch that restores intestinal continuity and replaces the function of the large intestine. Unfortunately, nearly 50% of UC patients who undergo this surgery will develop *de novo* intestinal inflammation in the pouch, or pouchitis[2]. Symptoms of pouchitis mimic IBD, including urgency, diarrhea, bleeding, and abdominal pain. The etiology of pouchitis is not known and there are no FDA approved therapies. Treatment often entails chronic antibiotics and restarting immunosuppressive IBD therapies. A better understanding of the inflammatory response for this condition, as well as the anatomically distinct features of intestinal inflammation in the large intestine compared to the pouch, may provide new insights for the management of this disease.

Single-cell RNA sequencing (scRNA-seq) has enabled us to characterize tissue states at a high resolution to better understand human diseases. Surveys of the intestinal tissues have identified unknown subtypes of intestinal epithelial cells and cellular inflammation modules that predict treatment responsiveness[3–5]. In the field of IBD, this approach is providing new insights into these complex diseases and may provide opportunities to define new drug targets, therapeutic strategies and more personalized treatment options[6]. In support of region-specific properties of the intestinal epithelium, small intestinal organoids but not colonic organoids derived from individuals homozygous for the Crohn's disease variant of *ATG16L1* are

susceptible to TNF-α and respond to drugs targeting JAK/STAT and necroptosis signaling[7,8]. Although these findings highlight the importance of epithelial-intrinsic factors in determining the anatomical site affected in IBD subtypes, identifying differences in immune cells between the large and small intestine may also be necessary for explaining disease presentations specific to these regions.

Detailed analysis of lymphocyte differentiation in mice have shown that peripheral regulatory T cells (pTregs) and Th17 cell numbers are differentially regulated in these two anatomical sites in response to region-specific exposure or sampling of food antigens, metabolites, and microbes[9–12]. Homing signals, structural features inherent to the organ, and compartmentalized draining by lymph nodes can also contribute to the localization and function of immune cell subsets[13,14]. It is unclear whether the inflamed pouch harbors immune infiltrates similar to the inflamed colon, the organ it functionally replaces, or if it retains immune characteristics of the small intestinal origin for this new organ. A previous study using bulk RNA-Seq showed that, in addition to acquiring markers of the colon, the pouch is enriched for transcripts related to IL-17 signaling and dendritic cell maturation when compared with the small intestine[15]. Therefore, a detailed survey of immune cells may provide novel insight into mechanisms of inflammation and reveal unique therapeutic interventions.

Here, we utilized scRNA-seq to examine the immune cell types and their activation states from intestinal biopsies collected from the J-pouch as well as the colon of UC patients. Our goal was to identify shared and distinctive features of inflammation in the colon and J-pouch. By focusing on CD45+ leukocytes, we can obtain greater resolution of the immune cell landscape and utilize this data to generate cell type specific transcriptional signatures to deconvolute bulk RNA datasets. This enabled us to implicate an IL-1B signature in macrophages as being associated with inflammation and unresponsiveness to anti-integrin biologic therapies in UC patients.

RESULTS

Immune cell transcriptional profiling landscape of intestinal biopsies from the J-pouch and colon of ulcerative colitis (UC) patients.

To minimize batch effects and streamline processing, we first established a cryopreservation pipeline (See Methods) to store and analyze leukocytes from intestinal biopsy samples of UC patients (Supplementary Figure 1). Optimization of the freezing medium in particular enabled a robust yield of live immune cells that could be sorted on the flow cytometer for high quality transcriptome analysis (See Methods). Cells from all patient samples were sorted for CD45+ surface expression and sequenced by scRNA-seq on the 10X platform. Nearly 56,000 CD45+ cells were obtained from scRNA-seq of 26 frozen biopsies from inflamed ulcerative colitis (18,375 cells, *n*=11 samples), inflamed pouchitis (20,678 cells, *n*=10 samples) and uninflamed pouch (16,678 cells, *n*=5 samples). Two samples from inflamed UC patients were removed due to low quality of the sequencing reaction. Single cell transcriptomes from all samples were normalized and merged with Seurat version 3[16] (Supplementary Figure 2A). Over half of the profiled cells, 30,863 cells, were from T cell subsets, 21,324 cells from B cell subsets and the remaining 3,747 cells were myeloid subsets (Fig. 1A). From these 3 lineages we determined 6 major populations of cells including T cells, germinal center/follicular cells, plasma cells, cycling B cells, mast cells and monocyte/macrophage cells. These populations were defined by specific immune cell markers such as *CD3D, CD8A* and *CD4* for T cells, *BANK1, CD19* and *VPREB3* for GC/Follicular cells, *STMN1, MKI67* and *HMGB2* for cycling B cells, *MZB1*, *XBP1* and *DERL3* for plasma cells, *IL1B*, *LYZ* and *IL8* for Monocytes/Macrophages and *KIT*, *CPA3* and *CD9* for mast cells (Fig. 1B,D). The relative percentages of these 6 major populations per patient sample did not separate inflamed or uninflamed samples or pouch and UC samples by principle component analysis (PCA) (Supplementary Figure 2B-C), indicating that there are not major differences in the immune cell landscape between UC colon and pouch samples. When we examined inter-individual variation in relative percentages of the 6 major populations, there was a significantly greater ($p<0.01$) proportion of monocyte/macrophages in pouchitis and UC patient samples compared to the uninflamed pouch (Fig. 1C). This indicated that the

inflammatory condition was most consistently driven by differences in the myeloid cell compartment, especially in the monocyte/macrophage population.

Three monocyte/macrophage populations that are increased in inflamed patient samples

Further analysis of the myeloid cell clusters indicated at least 5 minor clusters of cells including three distinct types of monocyte/macrophages, mast cells and a small population of plasmacytoid dendritic cells (Fig. 2A). Differential analysis identified specific immune cell markers for each of these populations including *SOX4, MAFA* and *IERL5* (*SOX4*+/*MAFA*+), *IL1B, LYZ* and *S100A9* (*IL1B*+/*LYZ*+), *APOE, C1QA* and *DNASEIL3* (*APOE*+/*C1QC*+), *CCDC50, IRF4* and *PLAC8* (pDCs) and *KIT, CD69* and *CLU* (Mast Cells) (Fig. 2B). These markers led us to refer to the monocyte/macrophage populations as *SOX4*+/*MAFA*+, *IL1B*+/*LYZ*+ and *APOE*+/*C1QC*+ from here on. *SOX4*+/*MAFA*+ and *IL1B*+/*LYZ*+ Monocyte/macrophage populations were more abundant in patients with both inflamed UC and pouches compared to uninflamed pouches ($p<0.05$) (Fig. 2C). *APOE*+/*C1QC*+ Monocyte/macrophages and Mast cells had no significant differences (Fig. 2C). pDCs were not detected in uninflamed pouches and are small in number (Fig. 2C).

Gene expression profiles marking each of the monocyte/macrophage cell clusters indicated enrichment for unique gene pairs that varied within each cluster. In *SOX4*+/*MAFA*+ monocyte/macrophages, *SOX4* and *MAFA* were used as specific markers and used for *in silico* gating to identify cells with enriched expression for both of these genes (Fig. 2D-F). When examined in individual samples, the relative percentage of *SOX4*+/*MAFA*+ cells are significantly increased ($p < 0.01$) in inflamed pouch and UC samples compared to uninflamed pouches. Differential expression between pouch and UC patients in these cells indicated an increase in *IL1RN* and *LTB* in inflamed samples compared to uninflamed pouches (Fig. 2D). Increased relative percentage in inflamed samples was also true for *LYZ*+/*IL1B*+ cells in IL1B+/LYZ+ monocyte/macrophages and differentially expressed genes between pouch and UC included significant increases in *EREG*, *S100A8*, *CXCL2*, *VEGFA*, *IL8* and *APOC1* in inflamed samples (Fig. 2E). Additionally, *SPP1* an important macrophage marker for colorectal

cancer[17], was found to be differentially expressed in inflamed UC samples compared to uninflamed pouches. It was not, however, significant between inflamed and uninflamed pouches. *APOE*+/*C1QC*+ cells (Fig. 2F) were also significantly increased in inflamed samples ($p < 0.01$) and *HIF1A*, *PLAUR*, *APOC1*, *MMP9* and *IL7* all increased in inflamed samples. Interestingly, *CXCL8* and *DNASEIL3* increased specifically in pouchitis compared to UC inflamed samples. To further delineate transcriptional relationships between the monocyte/macrophage clusters we performed a pseudotime analysis restricted to the three monocyte/macrophage cell clusters (Fig. 2G). In contrast to the UMAP representation (Fig. 2A) a diffusion map projection with pseudotime maintains the difference between *SOX4*+/*MAFA*+ and *IL1B*+/*LYZ*+ monocyte/macrophages but suggests *APOE*+/*C1QC*+ cells as an intermediary population (Fig. 2E, black line). Specifically, *SOX4* is strongly associated with pseudotime as a marker of *SOX4*+/*MAFA*+ cells (Fig. 2H). *CLEC10A* and *VAMP8* are also associated with pseudotime but were not significantly associated with specific macrophage populations (Fig. 2H).

The *IL1B*+/*LYZ*+ monocyte/macrophages appear similar to butyrate-induced anti-microbial macrophages[18], which also has a signature characterized by the expression of calprotectin *S100A8/A9*. The expression of *APOE* and *C1QC* indicate those monocyte/macrophages could have a more phagocytic/efferocytotic phenotype[19,20]. In addition to *SOX4* and *MAFA*, *SOX4*+/*MAFA*+ monocyte/macrophages also express TREM1 and CXCL10 (IP-10) (Supplementary Figure 3) but otherwise express transcripts that are not associated with known macrophage functions. Hence, we identify here 3 types of related monocyte/macrophage cell states that are all increased in the inflamed samples regardless of large or small intestine origin.

Specific T cell subsets differ according to patient inflammation status and disease

Considering T cells comprised the largest cluster of cells in 25 of the 26 samples profiled we performed further clustering and differential expression analysis to characterize T cell subsets (Supplementary Figure 4A). Specifically, 12 clusters of T cells were identified and

characterized by expression of *IFNG, CD8, FOXP3, IL2, ATF3, IL7, TNF, CCL5, GZMB, TOX2* (Fig. 3A and Supplementary Figure 4A-B). From these subsets we find a cluster of *FOXP3*+ T cells (Tregs) increased in inflamed UC and pouch samples compared to uninflamed pouches (Fig. 3B, Supplementary Figure 4C). Naïve and activated CD8+ cells were increased in relative percentage in pouch samples compared to inflamed UC samples while *CD8*+ *NR4A2*+ cells were generally higher in uninflamed pouches compared to inflamed pouch and UC samples (Fig. 3B). For the other T cell subsets that were identified the relative percentages were not significantly different between the patient groups (Supplementary Figure 4D).

The marked expansion of *FOXP3*+ T cells in inflamed samples was consistent with a previous report whereby *FOXP3*+ regulatory T cells also expressed TNF[3]. Here, we find that expression of *BATF* is also an important feature of these cells (Fig. 3C) and *in silico* gating of *FOXP3*+/*BATF*+ expression in T cells clearly shows an increase in inflamed pouch and UC samples compared to uninflamed pouches (Fig. 3C). Differential expression analysis of the *FOXP3*+/*BATF*+ cells indicated a number of transcriptional changes between uninflamed pouches, pouchitis and inflamed UC including an increase in *TRBC1*, *TRBC2, RACK1, ANXA1* and *CCL5* in pouchitis samples compared to UC. Given the importance of *FOXP3* expression in these cells we confirmed their presence by staining for FOXp53 nuclear expression (see methods) in tissue sections from uninflamed pouch (n=5) and pouchitis (n=10) patients (Fig. 3D). The relative percentage of *FOXP3*+ cells in pouchitis patients again was greater than in the uninflamed pouches (p=0.17). In contrast, both *CD8*+ and naïve *CD8*+ T cells were less represented in the colon samples from inflamed UC patients compared to the pouch samples, regardless of inflammation status (Fig. 3B). Within these CD8+ populations *in silico* gating of *CD8*+/*IL2*+ expression in T cells identified differences between inflamed UC and pouch patients regardless of inflammation (Fig. 3E). *IL2* expression was identified as a marker for *CD8*+ and naive *CD8*+ T cell subsets (Fig. 3A). Additionally, differential expression analysis of the *CD8*+/*IL2*+ cells indicated *IL2*, *CCL4L2*, *CCL5*, *TRBC2*, *XCL2* and *IGKC* are all increased in both pouchitis and uninflamed pouch compared to inflamed UC (Fig. 3E). One possibility is that this difference between pouch and colon may reflect the increased proportion

of CD8+ T cells observed in the ileum compared with colon[21,22]. Hence, we identified here *FOXP3+BATF+* T cells as being the most increased population in inflamed samples, whereas CD8+ cells in general are more abundant in the pouch than in colon samples regardless of inflammation state.

B cell subsets are similar across disease types

Recently, intestinal inflammation in UC was reported to be associated with increased anti-commensal IgG, which could induce IL-1B by engaging Fcγ receptors on macrophages[23] indicating a role for B cells in pathogenesis. Despite their high frequency in many of the patient samples profiled, B cell subsets clustered into only 5 clusters across 26 patient samples (Supplementary Figure 5A). These subsets include cycling B cells, follicular cells, germinal center cells and two types of plasma cells which differ in *NFKBIA* expression (Supplementary Figure 5A). Traditional B cell markers and differentially expressed transcripts were used to identify these subtypes including *STMN1, MKI67, BANK1, LMO2, LY9, MZB1 and XPB1* (Supplementary Figure 5B). While there is a slight increase in plasma cell percentages in inflamed UC samples compared to inflamed and uninflamed pouches, there were no other significant differences in B cell states between the patient groups (Supplementary Figure 5C).

Validation of inflammation associated immune cell populations in public datasets of ulcerative colitis and Crohn's disease patient samples.

FOXP3+ Tregs may be induced or maintained by intestinal antigen presenting cells such as macrophages and dendritic cells[24]. To investigate this relationship further, we compared the relative percentage of *FOPX3+/BATF+* T cells and each of the specific monocyte/macrophages subsets as defined by their respective markers *SOX4*, *MAFA*, *IL1B*, *LYZ* and *APOE*, *C1QC* by linear regression (Fig. 4A). While, all three populations were significantly associated, the *SOX4+/MAFA+* cells were most strongly associated (R_2=0.388). *TREM1* is expressed by *SOX4+/MAFA+* monocyte/macrophage cells and can be induced by retinoic acid[25] which also

induces *FOXP3*+ Treg differentiation. However, apart from *CXCL10* expression, these cells do not exhibit many other features of immune activation (Supplementary Figure 3A).

Recently, studies from Smillie[3] et al. and Martin[26] et al. have provided additional datasets for single cell analysis of IBD subsets in UC and Crohn's Disease. We compared the 22 immune cell populations identified in this study with those public datasets. Based on the expression profiles of T cell subsets, many T cell populations were highly correlated with at least one other labeled T cell subset from Martin[26] or Smillie[3] et al., $r > 0.6$, with the exception of activated CD4 cells which did not correlate in Martins et al., and CD4+ cells in Smillie et al. (Fig. 4B,C). *IL1B*+/*LYZ*+, *APOE*+/*C1QC*+ monocyte/macrophages, mast cells and pDCs were also highly correlated with named populations "Inflammatory Monocytes" and "Resident Macrophages" from both public datasets (Fig. 4B, C). However, *SOX4*+/*MAFA*+ monocyte/macrophages were not strongly correlated in either of the two datasets, $r < 0.4$. It is possible that CD45+ enrichment of immune cells enabled us to identify this monocyte/macrophage population that was not previously detected. In B cells many of the subsets were correlated with named populations from both Martin[26] and Smillie[3] et al. including plasma cells, germinal centers, cycling B cells and follicular cells, $r > 0.6$ (Fig. 4B, C).

After confirming the identify of *FOXP3*+ regulatory T cells and *IL1B*+/*LYZ*+ monocyte/macrophages populations in public datasets, we wanted to validate the relationship of these cell subsets in inflammation. In both CD and UC patient samples, we found that *FOXP3*+/*BATF*+ regulatory T cells were significantly increased in inflamed/involved compared to non-inflamed and healthy patient samples respectively (Fig. 4D,E). We did not find major differences in the percentage of *IL1B*+/*LYZ*+ monocyte/macrophage cells in the data from Smillie[3] et al., which profiled inflamed UC and paired non-inflamed UC samples (n=18) and healthy samples (n=12) (Fig. 4D). However, CD patients from Martin[26] et al. with active inflammation (n=11) did exhibit significant increases in *IL1B*+/*LYZ*+ cell subsets compared to matched uninvolved tissue (Fig. 4E). No major differences between inflamed and uninflamed samples were found for *APOE*+/*C1QC*+ monocyte/macrophages (Supplementary Figure 6). We could not detect *MAFA* in either dataset so we used *MAFB* which was also a marker.

266 However, even *SOX4*+/*MAFB*+ cell populations were scarce in either datasets and did not allow
267 us to determine if these cells were associated with inflammation (Supplementary Figure 6).
268 Hence, we find that increased abundance of *FOXP3*+/*BATF*+ T cells is a consistent feature of
269 inflammation in both UC and CD patients, whereas enrichment of specific
270 monocyte/macrophage subsets could be more context-dependent.
271
272 **Prioritizing inflammatory markers in a large cohort of IPAA patients**
273 We extracted 453 non-overlapping signature genes by differential expression and outlier
274 analysis[27] (Fig. 5A, Supplementary Table 1) as a signature matrix for the 12 T cell, 5 B cell and
275 5 myeloid cell subsets identified by scRNA-seq. We also extracted gene expression data for
276 genome wide association study (GWAS) risk genes that are associated with IBD[3] from our
277 scRNA-seq signature (Fig. 5A, Supplementary Figure 7). 17 of the GWAS-implicated IBD risk
278 alleles were associated with specific immune cells populations (Fig. 5A). For example, *IFNG*
279 was associated with CD8+ T cells, *CCL20* was associated with Th17 cells and *LY9* was
280 associated with follicular B cells. 45 other IBD-associated genes were also found in the scRNA-
281 seq dataset but were not found to be significant markers of our immune cell signatures
282 (Supplementary Figure 7) indicating that expression of these genes was not specific to a
283 particular immune cell population.
284 After generating an immune cell signature matrix, we examined the expression of these
285 genes in a microarray dataset from a larger study of IPAA patients (n=250) with active pouchitis
286 (PI), uninflamed pouches (NP) and familial adenomatous polyposis (FAP)[28]. This dataset also
287 included 16S rRNA microbial profiling data from paired biopsies. Based on the 453-gene
288 signature matrix generated by our single cell data, there were no appreciable differences
289 between groups of IPAA patient samples by PCA (Fig. 5B). However, we found greater
290 separation of patient samples in relation to the composite inflammation score (ISCORE)[28].
291 Patients with the highest ISCORE contributed most to the separation in PCA space (Fig. 5B).
292 We therefore split the patient samples according to the ISCORE values into a low (ISCORE <
293 2, n=223) and high (ISCORE > 2, n=50) inflammation group and performed differential

expression analysis by limma[29] version 3.38.3 limited to the 453 gene signature from our single cell dataset. The most differentially expressed transcripts in inflamed patient samples were related to the proinflammatory *IL1B*+/*LYZ*+ monocyte/macrophages, marked by *IL1B, S100A8, IL1RN* and *CXCL2* (Fig. 5C). We also found that expression of the inflammatory marker *IL1B* was significantly related to ISCORE (Fig. 5D). To determine if there are microbial associations with this set of host-transcripts, we employed sPLS regression to identify microbial taxa most associated with the *IL1B*+/*LYZ*+ monocyte/macrophages signature genes. We find that the expression of these genes is positively correlated with the abundance of *Escherichia, Bacteroides, Faecalibacterium* and inversely correlated with abundance for the order *Clostridiales* (Fig. 5E). Hence, there may be particular macrophage-microbe interactions that drive this anti-microbial IL-1B signature in inflammatory macrophages specifically during inflammation of the pouch.

Evaluating response to clinical therapies and inflammation status in ulcerative colitis

In order to identify cytokine signaling networks and immunoregulatory mechanisms between the 22 immune cell subsets in UC, we next investigated receptor-ligand pair networks between cells[30] to construct a cellular interaction network (Fig. 6A). Using a curated database of receptor-ligand interactions from cellPhoneDB[31], we identified pairs of interacting cell subsets based on our 453 gene signature matrix. Across the 22 immune cell subsets we identified 629 significant interactions between receptor-ligand pairs. *IL1B*+/*LYZ*+ and *APOE*+/*C1QC*+ monocyte/macrophages had the most interacting pairs and are the largest nodes of this network by number of connections, with many significant interactions between the two cell types. Additionally, Th17 cells are an important interacting node with these macrophage populations (Fig. 6A). The interactions between Th17 cells and *IL1B*+/*LYZ*+ monocyte/macrophages and *APOE*+/*C1QC*+ monocyte/macrophages include activity involving the chemokines *CCL3*, *CCL4*, *CCL5* and *CCL20* with the receptors *CCR1*, *CCR4*, *CCR5*, *CCR6* (Fig. 6B). Costimulatory molecule interactions with their ligands such as *CTLA-4, ICOS, PD-1* and *CD40* were also significant between Th17 and *FOXP3*+ T cells with the *IL1B*+/*LYZ*+ and

322 *APOE*+/*C1QC*+ monocyte/macrophages populations (Fig. 6B). Some of the other notable
323 interactions relate to cytokines such as *TNF* and *CSF*, which are important in disease
324 pathogenesis[32]. In summary, this approach enabled us to determine that *IL1B*+/*LYZ*+
325 monocyte/macrophages interactions with Th17 cells could be an important component of the
326 intestinal immune response during inflammation for these UC patients.

327 Several new therapeutic agents developed for treating UC patients are designed to
328 block immune cell interactions. Etrolizumab and Vedolizumab target the α4β7 integrin, and
329 Golimumab targets TNFα, but there is considerable heterogeneity in patient responsiveness
330 that is poorly understood. We next assessed if the cell specific signature of immune cell subsets
331 could distinguish between responders and non-responders for 3 different treatments for UC,
332 Vedolizumab[33] (GSE73661), Etrolizumab[34] (GSE72819), and Golimumab[35] (GSE92415). We
333 examined differential expression between responders and non-responder in for the 453-gene
334 signature matrix for these treatment studies. Transcripts associated with *IL1B*+/*LYZ*+
335 monocyte/macrophages were the most significantly different between responders and non-
336 responders for Vedolizumab treatment. The non-responders were most enriched in transcripts
337 for the proinflammatory *IL1B*+/*LYZ*+ monocyte/macrophages subset (Fig. 6C,D), indicating
338 that the presence of these macrophages could be an indicator of resistance to α4β7 integrin
339 blockade. In addition to *IL1B*, calprotectin components *S100A8/A9* were more highly expressed
340 in non-responders. However, there is considerable heterogeneity, in that approximately 50% of
341 non-responders have high expression of *IL1B*+/*LYZ*+ monocyte/macrophages transcripts (Fig.
342 6D). Non-responders to Etrolizumab treatment also exhibited higher expression of
343 proinflammatory genes like *IL1B, IL1RN* and *S100A9* compared to responders (Supplementary
344 Figure 8). Golimumab non-responders, while still slightly enriched for expression of these
345 transcripts, are less strikingly associated with *IL1B*+/*LYZ*+ monocyte/macrophages transcripts
346 (Supplementary Figure 8), perhaps reflecting the different mechanism of action. Hence, we find
347 that a proportion of non-responders to α4β7 integrin blockade in UC patients are associated
348 with increased transcripts for an inflammatory monocyte/macrophage population that expresses
349 an anti-microbial signature.

DISCUSSION

In this study, we found that inflammation in the ileal-anal J pouch, a novel organ created from ileal tissue has an inflammatory landscape similar to the colon of ulcerative colitis patients. We identified *FOXP3+/BATF+* T cells and 3 different monocyte/macrophage populations (*IL1B+/LYZ+*, *SOX4+/MAFA+* and *APOE+/C1Q+*) with inflamed tissues in both UC and pouchitis. Of these cells, the *IL1B+/LYZ+* monocyte/macrophages were the most highly connected cell type in the inflammatory network and their signature was associated with the lack of responsiveness to α4β7 integrin blockade and an increased abundance of *Bacteroides* and *Escherichia* bacterial populations. We hypothesize that the increased activation of these *IL1B+/LYZ+* monocyte/macrophages may be representative of a different intestinal inflammation state that is indicative of an immune response that cannot be modulated by α4β7 integrin blockade.

Our initial goal was to compare immune infiltration for the J-pouch with the colon, as two organs performing a similar function but with the J-pouch originating from the small intestine. This analysis concludes that the inflammatory response for pouchitis and UC is remarkably similar despite the different origin tissues. While the pouch has more CD8+ T cells of different phenotypes, which may reflect the increased proportion of CD8+ T cells observed in the ileum compared with colon[21,22], this is not significantly altered by the inflammatory response. This data supports previous studies indicating that pouchitis and UC are driven by similar inflammatory mechanisms[15] and may therefore respond to similar therapeutics[36–40]. Notably, we did not characterize the CD45+ immune cells of the pouch for patients with FAP, who develop pouchitis less frequently and may reveal features unique for the UC associated pouch even without the presence of inflammation. Recently, secondary bile acids and associated microbes were found to distinguish UC and FAP pouches, and may result in the pro-inflammatory conditions preceding pouchitis in UC patients[41]. Efforts are underway in determining the distinct roles of secondary bile acids and butyrate, both of which are byproducts of similar bacterial taxa that mediate Th17 and Treg polarization, and

discerning the action of these metabolites on antigen presenting cells versus T cells remains an important area of research[11,41–45]. Thus, it is important to identify any association between the *IL1B*+/*LYZ*+ monocyte/macrophages and other metabolites such as bile acids beyond butyrate[18].

The relationship between microbes and antimicrobial macrophages is particularly relevant to the pathogenesis of IBD. ScRNA-seq of human monocyte derived macrophages treated with butyrate had previously been shown to induce an antimicrobial signature through *HDAC3* including upregulation of autophagy-related processes[18]. Here we provide evidence that macrophages with an overlapping antimicrobial signature can directly be identified from intestinal biopsies of UC patients. This observation may reflect the recruitment of monocytes to the gut where they differentiate into macrophages to counteract a breach in the epithelial barrier, a characteristic of IBD patients who are colonized by pro-inflammatory bacteria related to *Bacteroides* and *Escherichia* species[46–48]. In contrast to healthy individuals, local cytokine responses and inefficient autophagy may prevent macrophages from resolving the breach in the barrier, leading to a detrimental pro-inflammatory effect of macrophages[49]. Consistent with this possibility, our previous work indicates that antimicrobial monocytes and macrophages recruited to the gut are beneficial when damage to the colon is temporary, even with an inflammatory cytokine signature exacerbated by the absence of autophagy[50–52].

The most consistent finding between our scRNA-seq data and the meta-analysis of data from public datasets is the expansion of *FOXP3*+/*BATF*+ Tregs in actively inflamed IBD. Expression of *BATF* in FOXP3+ Tregs is indicative of tissue residency[53]. In the visceral adipose tissue, FOXP3+ Tregs require *BATF* for differentiation downstream of *ST2* and *PPARG* activity[54]. In the intestine, *BATF* regulates expression of *CCR9* and a4b7 and *BATF* deficient mice have reduced effector as well as FOXP3+ T cells in the intestine[55]. Hence, *BATF* is likely an important transcription factor for the differentiation and recruitment of FOXP3+ Tregs to the intestinal tissues during inflammation. Notably, a recent report on scRNA-seq analysis of immune cell populations in immune checkpoint inhibitor-induced colitis also reveals the persistence and expansion of Tregs[56]. The increased accumulation of

406 FOXP3+ Tregs in the inflamed colon is likely driven by the need to restrain inflammation, but
407 why these Tregs are not successful in controlling inflammation requires further study. One
408 possibility may be that the presence of inflammatory monocyte/macrophage populations can
409 somehow inhibit the appropriate function of these regulatory cells.

410 We also observe expansion of *APOE*+/*C1QC*+ monocyte/macrophages with a
411 phagocytic signature in both the inflamed pouch and colon, which are reminiscent of the
412 tumor associated macrophage (TAM) populations recently described in colorectal cancer
413 (CRC) patients[57]. In that study, the C1QC+ macrophages were found to be closely connected
414 with IL1B+ macrophages, which we also find in this study. This indicates that there are some
415 similar characteristics between the myeloid infiltration observed in CRC and UC. However,
416 the role of these macrophages beyond having a phagocytic signature remain unclear and will
417 require further study. Notably, we did not observe the *SPP1*+ macrophage described in CRC
418 patients[17,57].

419 We had previously found increase in Th17 cells in inflamed biopsies[58,59] linked by
420 expression of *SAA1* with *Bacteroides* abundance, but this was by flow cytometry and
421 intracellular cytokine staining. Serum amyloid A (SAA) proteins produced by intestinal
422 epithelial cells can drive differentiation of inflammatory Th17 cells according to the tissue
423 environment[60], however expression of SAA proteins was not detected in the present study
424 because we selected for immune cells. We also do not observe significantly more Th17 cells
425 by transcriptional signature (Supplementary Figure 4D). Nonetheless, this population of cells
426 is highly connected with the *IL1B*+/*LYZ*+ and *APOE*+/*C1QC*+ populations that are expanded
427 in inflamed samples and hence their activity could be highly dependent on the interaction
428 with these macrophages. Causal relationships between these populations may be discerned in
429 the future through *in vitro* co-culture assays but purifying specific populations of these
430 immune cells will entail surgical specimens rather than the mucosal pinch biopsies utilized in
431 this study.

432 IL-1B release can be triggered by activating *NLRP3* and other inflammasomes in
433 macrophages exposed to invasive microbes. Elegant experiments examining very early onset

IBD (VEOIBD) patients and mouse models genetically deficient in IL-10 signaling indicate that inflammasome-triggered IL-1B production by macrophages polarizes CD4+ T cells that mediate colitis[61,62]. Blocking IL-1B signaling was effective in two IL10R-deficient patients with treatment-refractory disease[62], suggesting that macrophage-T cell interactions (Fig. 6A-B) drive disease in the absence of IL-10 and other immuno-suppressive Treg effectors. This would be consistent with predictions from the receptor ligand analysis performed in this study (Fig. 6). If the presence of *IL1B*+ macrophages are indicative of unresponsiveness to α4β7 integrin blockade as suggested by our results, therapies that target *IL1B* itself or JAK/STAT inhibitors that broadly target signaling downstream of IL-1B-induced cytokines[63] may be promising alternatives for UC patients with this signature. Detailed analysis of tissue from patients receiving JAK/STAT inhibitors will be highly informative.

In conclusion, this work utilizes scRNA-seq to identify unique features of pouchitis and a specific population of *IL1B*+ macrophages that could potentially be targeted in a subset of UC patients who are not responding to treatment with α4β7 integrin antagonists. Hence, this study provides an example of how utilizing precision medicine to identify changes in cell proportions, gene expression and cell-cell signaling by scRNA-seq, followed by further analyses of publicly available datasets, could be used to improve our understanding of individual patient responsiveness to IBD therapies and provide a hypothesis for alternative treatment options.

METHODS

Study Participants

Participants were recruited and consented and are part of an institutional review board–approved study (S12-01137; "Mucosal immune profiling in patients with inflammatory bowel disease") by NYU Langone Health. We identified 15 patients with a J-pouch and 13 patients with UC (Supplementary Table 2). All J-pouch patients had preoperative UC with 14 (93%) and 1 (7%) undergoing an IPAA for medically refractory

461 disease and colitis-associated neoplasia, respectively. Of J-pouch patients, 10 (67%) had
462 endoscopic evidence of inflammation (endoscopic PDAI ≥2) referred to as pouchitis and 5
463 (33%) had endoscopically normal appearing pouches referred to as uninflamed pouches
464 (Supplementary Table 2). All UC patients had moderate to severe endoscopic activity
465 (endoscopic Mayo ≥2). Patients with UC or a J-pouch at the Inflammatory Bowel
466 Disease Center at NYU Langone Health, New York, were approached for recruitment
467 on presentation for routine endoscopy (pouchoscopy, colonoscopy, or flexible
468 sigmoidoscopy) performed for disease activity assessment. Potential participants were
469 excluded if they were unable to or did not consent to provide tissue. The endoscopic
470 appearance determined the inflammatory activity. UC patients were limited to those
471 with active inflammation denoted by an Mayo endoscopic subscore of ≥2[64]. J-pouch
472 patients were stratified into an endoscopic pouchitis cohort for those with an pouchitis
473 disease activity index (PDAI) endoscopic subscore ≥2 or a normal J-pouch cohort for
474 those with an PDAI endoscopic subscore <2[65]. Further patient details and stratification
475 are described in Supplementary Table 2.
476
477 *Biopsies*
478 Approximately four to ten mucosal pinch biopsies were obtained from each patient. For
479 UC patients, all biopsies were obtained from the rectum. For J-pouch patients, all
480 biopsies were obtained from the pouch body or inlet. If active endoscopic inflammation
481 was present, this area was targeted for biopsy. For each location sampled, one biopsy
482 was collected for standard histopathology assessment and read by two expert
483 pathologists for the PDAI histology subscore and histologic pouch activity score
484 (PAS)[65,66].
485

Patient metadata

At endoscopy, clinical data was collected including demographics, initial IBD subtype and phenotype, smoking status, the presence of primary sclerosing cholangitis (PSC), extra-intestinal manifestations, and comorbidities, age and indication for IPAA, previous and current medication exposures, and clinical indices of disease activity including the partial Mayo score[64] for patients with UC and PDAI clinical subscore for patients with a J-pouch[65] (Supplementary Table 2).

Biopsy specimen processing

All biopsies were collected in ice cold complete RPMI 1640 (10% FBS, 100x penicillin/streptomycin/glutamine, 50uM 2-mercaptoethanol, Sigma) during endoscopy and subsequently cryopreserved in freezing media (90% FBS + 10% DMSO) for long-term storage. Cryopreserved biopsies were gently thawed at 37°C and enzymatically digested in collagenase VIII (Sigma) and DNase (Sigma) for 1h to obtain a single cell suspension. After live/dead cell staining with near-IR stain (Invitrogen), cell surface markers were labeled with the following antibodies: CD45 PE-Cy7, CD3 PerCP-Cy5.5, CD19 PE, CD14 FITC, and CD16 Pacific Blue (BioLegend). Sorted CD45+ cellular suspensions were isolated using the Sony SY3200 cell sorter and prepared for single-cell RNA sequencing.

Single cell library and sequencing

From pinch biopsies all samples were sorted and CD45+ cellular suspensions were loaded on a 10x Genomics Chromium instrument to generate single-cell gel beads in emulsion (GEMs). Approximately 10,000 cells were loaded per channel. Single-cell RNA-Seq libraries were prepared using the following Single Cell 3' Reagent Kits v2:

Chromium™ Single Cell 3' Library & Gel Bead Kit v2, Single Cell 3' Chip Kit v2, and i7 Multiplex Kit (catalog# PN-120237, PN-120236, # PN-120262, 10x Genomics)[67] and following the Single Cell 3' Reagent Kits v2 User Guide (Manual Part # CG00052), Rev A. Libraries were run on an Illumina HiSeq 4000 as 2 × 150 paired-end reads, one full lane per sample, for approximately >90% sequencing saturation.

Single cell analysis pipeline

The Cellranger software suite (https://support.10xgenomics.com/single-cell-gene-expression/software/pipelines/latest/what-is-cell-ranger) from 10X was used to demultiplex cellular barcodes, align reads to the human genome (GRCh38 ensemble, http://useast.ensembl.org/Homo_sapiens/Info/Index) and perform UMI counting. From filtered counts Seurat[16] version 3.1.3 was used to process the single cell data including dimension reduction, UMAP representation and differential expression to identify cell type specific markers and differentially expressed genes between pouch and UC conditions by a Wilcox test. All single cell processing steps, code and gene expression tables are described in detail on our github at https://github.com/ruggleslab/Pouch. We also used additional single cell analysis software including diffusion map and pseudotime analysis from the R package Slingshot[68] version 1.0.0.

Immunohistochemistry staining for FOXP3+ cells

Image panels were acquired with ×10 lens using an Olympus BX53 microscope equipped with an Olympus DP27 digital color camera (Olympus, Center Valley, PA, USA). FOXp53 nuclear expression, stained with 3,3-Diaminobenzidine (DAB) was digitally quantified by QuPath[69] using hematoxylin as a background stain. Areas of

interest were drawn with the line or polygon drawing tool. *FOXP3* cells and background immune cells were annotated. The images were thresholded using a binary categorization of positive (DAB, brown stain) and negative (blue stain). Default software settings were used for the final analysis with the help of cell analysis, positive cell detection command as previously published[70]. The measurement table was then exported to excel spread sheet for statistical analysis.

Generating Receptor-ligand networks

Receptor-ligand networks were generated using the software CellPhoneDB[31] using the default databases and methods as described in their documentation (https://github.com/Teichlab/cellphonedb).

DATA AND CODE AVAILABILITY

Raw sequence data are deposited in the NCBI Sequence Read Archive under BioProject accession number XXX and gene expression omnibus (GEO) accession number GSEXXX. All processing was performed in R[71] version 3.5.1 and complete analysis scripts can be found on github at https://github.com/ruggleslab/Pouch .

Acknowledgements

We wish to thank the NYU School of Medicine Flow Cytometry and Cell Sorting, Microscopy, Genome Technology, and Histology Cores for use of their instruments and technical assistance (supported in part by National Institute of Health (NIH) grant P31CA016087, S10OD01058, and S10OD018338). **Funding:** This research was supported by the Division of Intramural Research, National Institute of Allergy and Infectious Diseases, National Institutes of Health (NIH) and NIH grants DK103788 (K.C. and P.L.), AI121244

(K.C.), HL123340 (K.C.), DK093668 (K.C.), AI130945 (P.L. and K.C.), R01 HL125816 (K.C.), R01 AI140754 (K.C.), HL084312, AI133977 (P.L.). Pilot award from the NYU CTSA grant UL1TR001445 from the National Center for Advancing Translational Sciences (NCATS) (K.C., P.L.), pilot award from the NYU Cancer Center grant P30CA016087 (K.C.). This work was also supported by the Faculty Scholar grant from the Howard Hughes Medical Institute (K.C.), Crohn's & Colitis Foundation (K.C.), Merieux Institute (K.C.), Kenneth Rainin Foundation (K.C.). K.C. is a Burroughs Wellcome Fund Investigator in the Pathogenesis of Infectious Diseases.

Author contributions: Design of experiments, data analysis, data discussion, and interpretation: J.C.D., J.A., S.C., K.V.R., D.H., K.C. and P.L.; primary responsibility for execution of experiments: A.M.H., J.D.L., Single cell analysis: J.C.D., K.V.R. All authors discussed data and commented on the manuscript.

Declaration of interests: K.C. receives research funding from Pfizer and Abbvie; P.L. receives research funding from Pfizer; J.A. receives research funding from BioFire Diagnostics. K.C. has consulted for or received an honorarium from Puretech Health, Genentech, and Abbvie; P.L. consults for and has equity in Toilabs. K.C. has provisional patents, U.S. Patent Appln. No. 15/625,934 and 62/935,035. P.L. is a federal employee. J.A. has consulted for or received an honorarium from BioFire Diagnostics and Janssen.

REFERENCES

1. Shen, B. Acute and chronic pouchitis—pathogenesis, diagnosis and treatment. *Nature Reviews Gastroenterology & Hepatology* **9**, 323–333 (2012).
2. Dalal, R. L., Shen, B. & Schwartz, D. A. Management of Pouchitis and Other Common Complications of the Pouch. *Inflamm Bowel Dis* **24**, 989–996 (2018).

3. Smillie, C. S. *et al.* Intra- and Inter-cellular Rewiring of the Human Colon during Ulcerative Colitis. *Cell* **178**, 714-730.e22 (2019).

4. Haber, A. L. *et al.* A single-cell survey of the small intestinal epithelium. *Nature* **551**, 333–339 (2017).

5. Parikh, K. *et al.* Colonic epithelial cell diversity in health and inflammatory bowel disease. *Nature* **567**, 49–55 (2019).

6. Corridoni, D., Chapman, T., Antanaviciute, A., Satsangi, J. & Simmons, A. Inflammatory Bowel Disease Through the Lens of Single-cell RNA-seq Technologies. *Inflamm Bowel Dis* doi:10.1093/ibd/izaa089.

7. Matsuzawa-Ishimoto, Y. *et al.* An intestinal organoid-based platform that recreates susceptibility to T-cell-mediated tissue injury. *Blood* **135**, 2388–2401 (2020).

8. Matsuzawa-Ishimoto, Y. *et al.* Autophagy protein ATG16L1 prevents necroptosis in the intestinal epithelium. *J Exp Med* **214**, 3687–3705 (2017).

9. Xu, M. *et al.* c-MAF-dependent regulatory T cells mediate immunological tolerance to a gut pathobiont. *Nature* **554**, 373–377 (2018).

10. Sano, T. *et al.* An IL-23R/IL-22 Circuit Regulates Epithelial Serum Amyloid A to Promote Local Effector Th17 Responses. *Cell* **163**, 381–393 (2015).

11. Furusawa, Y. *et al.* Commensal microbe-derived butyrate induces the differentiation of colonic regulatory T cells. *Nature* **504**, 446–450 (2013).

12. Kim, K. S. *et al.* Dietary antigens limit mucosal immunity by inducing regulatory T cells in the small intestine. *Science* **351**, 858–863 (2016).

13. Esterházy, D. *et al.* Compartmentalized gut lymph node drainage dictates adaptive immune responses. *Nature* **569**, 126–130 (2019).

610 14. Habtezion, A., Nguyen, L. P., Hadeiba, H. & Butcher, E. C. Leukocyte
611 Trafficking to the Small Intestine and Colon. *Gastroenterology* **150**, 340–354
612 (2016).
613 15. Huang, Y. *et al.* Early Transcriptomic Changes in the Ileal Pouch Provide
614 Insight into the Molecular Pathogenesis of Pouchitis and Ulcerative Colitis.
615 *Inflamm Bowel Dis* **23**, 366–378 (2017).
616 16. Stuart, T. *et al.* Comprehensive Integration of Single-Cell Data. *Cell* **177**,
617 1888-1902.e21 (2019).
618 17. Lee, H.-O. *et al.* Lineage-dependent gene expression programs influence
619 the immune landscape of colorectal cancer. *Nature Genetics* **52**, 594–603
620 (2020).
621 18. Schulthess, J. *et al.* The Short Chain Fatty Acid Butyrate Imprints an
622 Antimicrobial Program in Macrophages. *Immunity* **50**, 432-445.e7 (2019).
623 19. Arnold, L. *et al.* CX3CR1 deficiency promotes muscle repair and
624 regeneration by enhancing macrophage ApoE production. *Nature*
625 *Communications* **6**, 8972 (2015).
626 20. Grainger, D. J., Reckless, J. & McKilligin, E. Apolipoprotein E Modulates
627 Clearance of Apoptotic Bodies In Vitro and In Vivo, Resulting in a Systemic
628 Proinflammatory State in Apolipoprotein E-Deficient Mice. *The Journal of*
629 *Immunology* **173**, 6366–6375 (2004).
630 21. Senda, T. *et al.* Microanatomical dissection of human intestinal T-cell
631 immunity reveals site-specific changes in gut-associated lymphoid tissues
632 over life. *Mucosal Immunol* **12**, 378–389 (2019).
633 22. Mowat, A. M. & Agace, W. W. Regional specialization within the intestinal
634 immune system. *Nature Reviews Immunology* **14**, 667–685 (2014).

635 23. Castro-Dopico, T. *et al.* Anti-commensal IgG Drives Intestinal
636 Inflammation and Type 17 Immunity in Ulcerative Colitis. *Immunity* **50**, 1099-
637 1114.e10 (2019).
638 24. Bain, C. C. & Mowat, A. M. Macrophages in intestinal homeostasis and
639 inflammation. *Immunological Reviews* **260**, 102–117 (2014).
640 25. Fontana, R. *et al.* Nuclear receptor ligands induce TREM-1 expression on
641 dendritic cells: analysis of their role in tumors. *OncoImmunology* **8**, 1554967
642 (2019).
643 26. Martin, J. C. *et al.* Single-Cell Analysis of Crohn's Disease Lesions Identifies
644 a Pathogenic Cellular Module Associated with Resistance to Anti-TNF Therapy.
645 *Cell* **178**, 1493-1508.e20 (2019).
646 27. Mertins, P. *et al.* Proteogenomics connects somatic mutations to signalling
647 in breast cancer. *Nature* **534**, 55–62 (2016).
648 28. Morgan, X. C. *et al.* Associations between host gene expression, the
649 mucosal microbiome, and clinical outcome in the pelvic pouch of patients with
650 inflammatory bowel disease. *Genome Biology* **16**, 67 (2015).
651 29. Ritchie, M. E. *et al.* limma powers differential expression analyses for
652 RNA-sequencing and microarray studies. *Nucleic Acids Res* **43**, e47–e47
653 (2015).
654 30. Ramilowski, J. A. *et al.* A draft network of ligand–receptor-mediated
655 multicellular signalling in human. *Nature Communications* **6**, 7866 (2015).
656 31. Efremova, M., Vento-Tormo, M., Teichmann, S. A. & Vento-Tormo, R.
657 CellPhoneDB: inferring cell–cell communication from combined expression of
658 multi-subunit ligand–receptor complexes. *Nature Protocols* **15**, 1484–1506
659 (2020).

660 32. Friedrich, M., Pohin, M. & Powrie, F. Cytokine Networks in the
661 Pathophysiology of Inflammatory Bowel Disease. *Immunity* **50**, 992–1006
662 (2019).
663 33. Arijs, I. *et al.* Effect of vedolizumab (anti-α4β7-integrin) therapy on
664 histological healing and mucosal gene expression in patients with UC. *Gut* **67**,
665 43–52 (2018).
666 34. Tew, G. W. *et al.* Association Between Response to Etrolizumab and
667 Expression of Integrin αE and Granzyme A in Colon Biopsies of Patients With
668 Ulcerative Colitis. *Gastroenterology* **150**, 477-487.e9 (2016).
669 35. Telesco, S. E. *et al.* Gene Expression Signature for Prediction of
670 Golimumab Response in a Phase 2a Open-Label Trial of Patients With
671 Ulcerative Colitis. *Gastroenterology* **155**, 1008-1011.e8 (2018).
672 36. Ferrante, M. *et al.* Efficacy of infliximab in refractory pouchitis and
673 Crohn's disease-related complications of the pouch: a Belgian case series.
674 *Inflamm. Bowel Dis.* **16**, 243–249 (2010).
675 37. Barreiro-de Acosta, M. *et al.* Efficacy of infliximab rescue therapy in
676 patients with chronic refractory pouchitis: a multicenter study. *Inflamm.*
677 *Bowel Dis.* **18**, 812–817 (2012).
678 38. Barreiro-de Acosta, M. *et al.* Efficacy of adalimumab rescue therapy in
679 patients with chronic refractory pouchitis previously treated with infliximab:
680 a case series. *Eur J Gastroenterol Hepatol* **24**, 756–758 (2012).
681 39. Bär, F. *et al.* Vedolizumab in the treatment of chronic, antibiotic-
682 dependent or refractory pouchitis. *Aliment. Pharmacol. Ther.* **47**, 581–587
683 (2018).

684 40. Ollech, J. E. *et al.* Ustekinumab Is Effective for the Treatment of Chronic
685 Antibiotic-Refractory Pouchitis. *Dig. Dis. Sci.* **64**, 3596–3601 (2019).
686 41. Sinha, S. R. *et al.* Dysbiosis-Induced Secondary Bile Acid Deficiency
687 Promotes Intestinal Inflammation. *Cell Host & Microbe* **27**, 659-670.e5 (2020).
688 42. Campbell, C. *et al.* Bacterial metabolism of bile acids promotes generation
689 of peripheral regulatory T cells. *Nature* **581**, 475–479 (2020).
690 43. Hang, S. *et al.* Bile acid metabolites control T H 17 and T reg cell
691 differentiation. *Nature* **576**, 143–148 (2019).
692 44. Song, X. *et al.* Microbial bile acid metabolites modulate gut RORγ +
693 regulatory T cell homeostasis. *Nature* **577**, 410–415 (2020).
694 45. Arpaia, N. *et al.* Metabolites produced by commensal bacteria promote
695 peripheral regulatory T-cell generation. *Nature* **504**, 451–455 (2013).
696 46. Kim, Y.-G. *et al.* The Nod2 Sensor Promotes Intestinal Pathogen
697 Eradication via the Chemokine CCL2-Dependent Recruitment of Inflammatory
698 Monocytes. *Immunity* **34**, 769–780 (2011).
699 47. Ramanan, D., Tang, M. S., Bowcutt, R., Loke, P. & Cadwell, K. Bacterial
700 sensor Nod2 prevents small intestinal inflammation by restricting the
701 expansion of the commensal Bacteroides vulgatus. *Immunity* **41**, 311–324
702 (2014).
703 48. Schirmer, M., Garner, A., Vlamakis, H. & Xavier, R. J. Microbial genes and
704 pathways in inflammatory bowel disease. *Nature Reviews Microbiology* **17**,
705 497–511 (2019).
706 49. Matsuzawa-Ishimoto, Y., Hwang, S. & Cadwell, K. Autophagy and
707 Inflammation. *Annual Review of Immunology* **36**, 73–101 (2018).

708 50. Marchiando, A. M. *et al.* A Deficiency in the Autophagy Gene Atg16L1
709 Enhances Resistance to Enteric Bacterial Infection. *Cell Host & Microbe* **14**,
710 216–224 (2013).
711 51. Martin, P. K. *et al.* Autophagy proteins suppress protective type I
712 interferon signalling in response to the murine gut microbiota. *Nature*
713 *Microbiology* **3**, 1131–1141 (2018).
714 52. Neil, J. A. *et al.* IFN-I and IL-22 mediate protective effects of intestinal viral
715 infection. *Nature Microbiology* **4**, 1737–1749 (2019).
716 53. Hayatsu, N. *et al.* Analyses of a Mutant Foxp3 Allele Reveal BATF as a
717 Critical Transcription Factor in the Differentiation and Accumulation of Tissue
718 Regulatory T Cells. *Immunity* **47**, 268-283.e9 (2017).
719 54. Vasanthakumar, A. *et al.* The transcriptional regulators IRF4, BATF and
720 IL-33 orchestrate development and maintenance of adipose tissue–resident
721 regulatory T cells. *Nature Immunology* **16**, 276–285 (2015).
722 55. Wang, C. *et al.* BATF is required for normal expression of gut-homing
723 receptors by T helper cells in response to retinoic acid. *J Exp Med* **210**, 475–
724 489 (2013).
725 56. Luoma, A. M. *et al.* Molecular Pathways of Colon Inflammation Induced by
726 Cancer Immunotherapy. *Cell* **0**, (2020).
727 57. Zhang, L. *et al.* Single-Cell Analyses Inform Mechanisms of Myeloid-
728 Targeted Therapies in Colon Cancer. *Cell* **181**, 442-459.e29 (2020).
729 58. Leung, J. M. *et al.* IL-22-producing CD4+ cells are depleted in actively
730 inflamed colitis tissue. *Mucosal Immunology* **7**, 124–133 (2014).

731 59. Tang, M. S. *et al.* Integrated Analysis of Biopsies from Inflammatory Bowel
732 Disease Patients Identifies SAA1 as a Link Between Mucosal Microbes with
733 TH17 and TH22 Cells. *Inflamm Bowel Dis* **23**, 1544–1554 (2017).
734 60. Lee, J.-Y. *et al.* Serum Amyloid A Proteins Induce Pathogenic Th17 Cells
735 and Promote Inflammatory Disease. *Cell* **180**, 79-91.e16 (2020).
736 61. Ip, W. K. E., Hoshi, N., Shouval, D. S., Snapper, S. & Medzhitov, R. Anti-
737 inflammatory effect of IL-10 mediated by metabolic reprogramming of
738 macrophages. *Science* **356**, 513–519 (2017).
739 62. Shouval, D. S. *et al.* Interleukin 1β Mediates Intestinal Inflammation in
740 Mice and Patients With Interleukin 10 Receptor Deficiency. *Gastroenterology*
741 **151**, 1100–1104 (2016).
742 63. Salas, A. *et al.* JAK–STAT pathway targeting for the treatment of
743 inflammatory bowel disease. *Nature Reviews Gastroenterology & Hepatology*
744 **17**, 323–337 (2020).
745 64. Schroeder, K. W., Tremaine, W. J. & Ilstrup, D. M. Coated Oral 5-
746 Aminosalicylic Acid Therapy for Mildly to Moderately Active Ulcerative Colitis.
747 *New England Journal of Medicine* **317**, 1625–1629 (1987).
748 65. Sandborn, W. J., Tremaine, W. J., Batts, K. P., Pemberton, J. H. & Phillips, S.
749 F. Pouchitis After Ileal Pouch-Anal Anastomosis: A Pouchitis Disease Activity
750 Index. *Mayo Clinic Proceedings* **69**, 409–415 (1994).
751 66. Heuschen, U. A. *et al.* Diagnosing Pouchitis. *Dis Colon Rectum* **45**, 776–786
752 (2002).
753 67. Zheng, G. X. Y. *et al.* Massively parallel digital transcriptional profiling of
754 single cells. *Nature Communications* **8**, 14049 (2017).

755 68. Street, K. *et al.* Slingshot: cell lineage and pseudotime inference for single-
756 cell transcriptomics. *BMC Genomics* **19**, 477 (2018).
757 69. Bankhead, P. *et al.* QuPath: Open source software for digital pathology
758 image analysis. *Scientific Reports* **7**, 16878 (2017).
759 70. Dowsett, M. *et al.* Assessment of Ki67 in Breast Cancer: Recommendations
760 from the International Ki67 in Breast Cancer Working Group. *J Natl Cancer Inst*
761 **103**, 1656–1664 (2011).
762 71. R Core Team. *R: A language and environment for statistical computing. R*
763 *Foundation for Statistical Computing*. (2018).
764

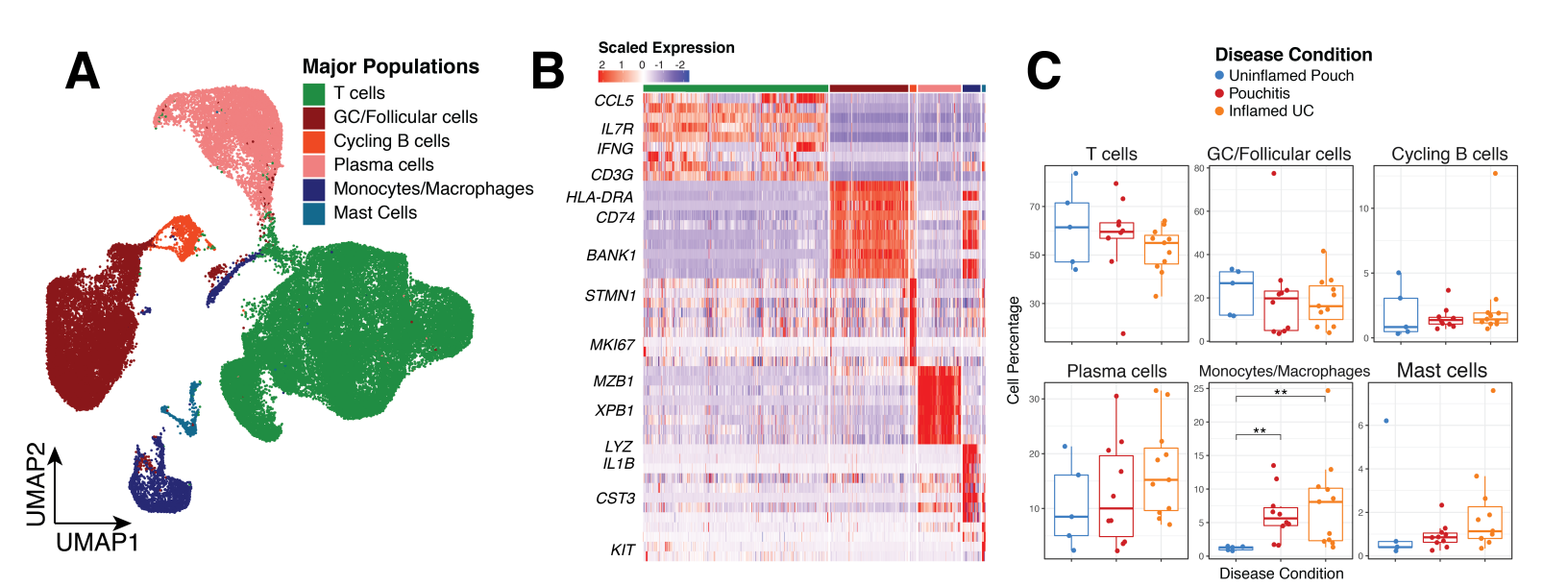
A
Major Populations
T cells
GC/Follicular cells
Cycling B cells
Plasma cells
Monocytes/Macrophages
Mast Cells
UMAP2
UMAP1
B
Scaled Expression
2 1 0 -1 -2
CCL5
IL7R
IFNG
CD3G
HLA-DRA
CD74
BANK1
STMN1
MKI67
MZB1
XPB1
LYZ
IL1B
CST3
KIT
C
Disease Condition
Uninflamed Pouch
Pouchitis
Inflamed UC
T cells
GC/Follicular cells
Cycling B cells
Plasma cells
Monocytes/Macrophages
Mast cells
Cell Percentage
**
**
Disease Condition

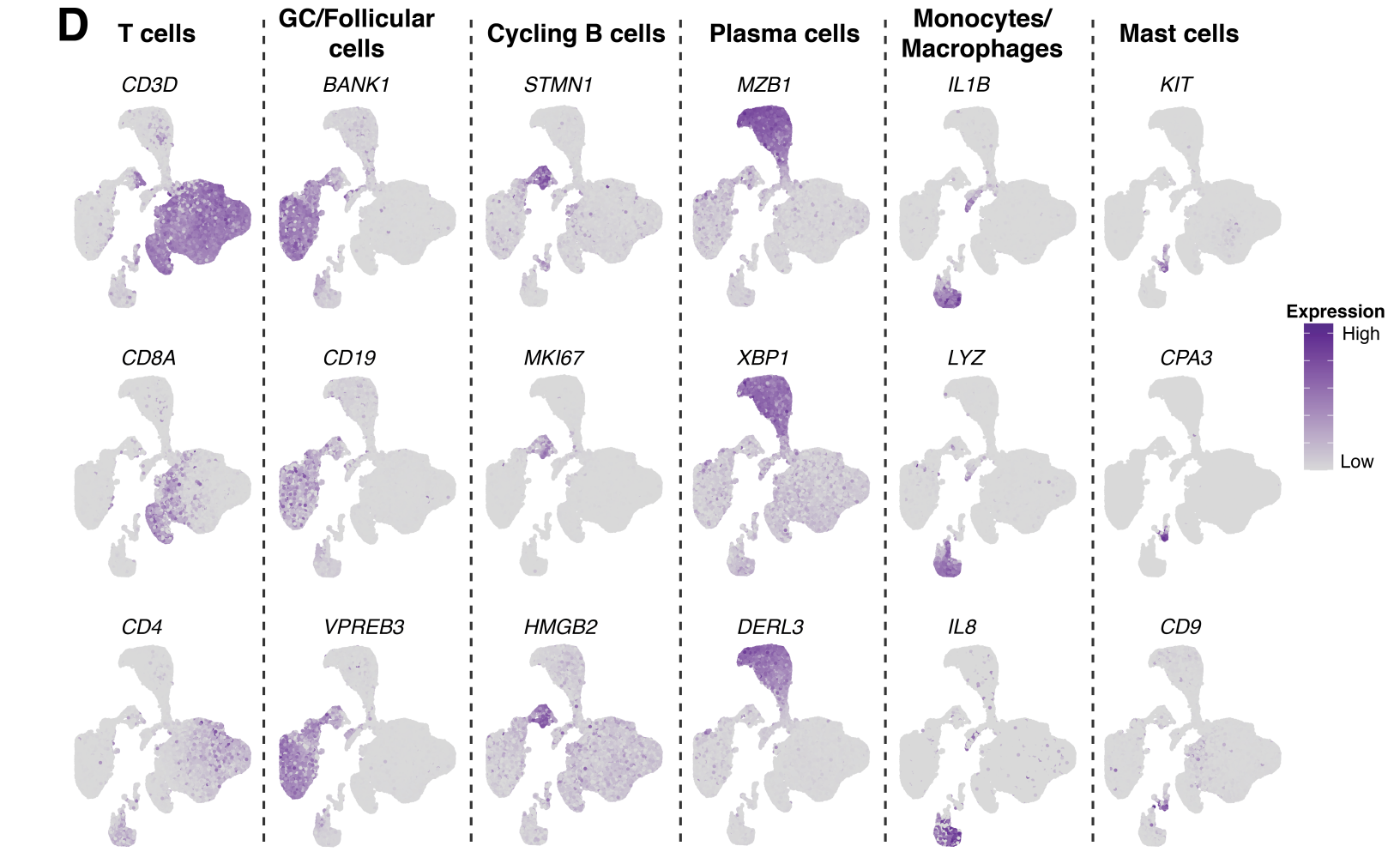
D
T cells
GC/Follicular cells
Cycling B cells
Plasma cells
Monocytes/ Macrophages
Mast cells
CD3D
BANK1
STMN1
MZB1
IL1B
KIT
CD8A
CD19
MKI67
XBP1
LYZ
CPA3
CD4
VPREB3
HMGB2
DERL3
IL8
CD9
Expression
High
Low

Figure 1. Immune cell landscape of frozen biopsy specimens obtained from the ileal-anal pouch and colon of ulcerative colitis patients. (A) Census of the major immune cell clusters and visualization by UMAP. (B) Heatmap of scaled expression profiles of the major immune cell clusters (C) Boxplots showing cell cluster frequency of the major populations as a percentage of total cells of each patient shown as individual datapoints, compared between patient groups. (D) Feature plots showing representative UMAP visualizations of normalized expression for marker genes enriched in the major cell types. Asterisks indicate significance testing for Wilcoxon ranked test, * = $p < 0.05$, ** = $p < 0.01$, *** = $p < 0.001$.

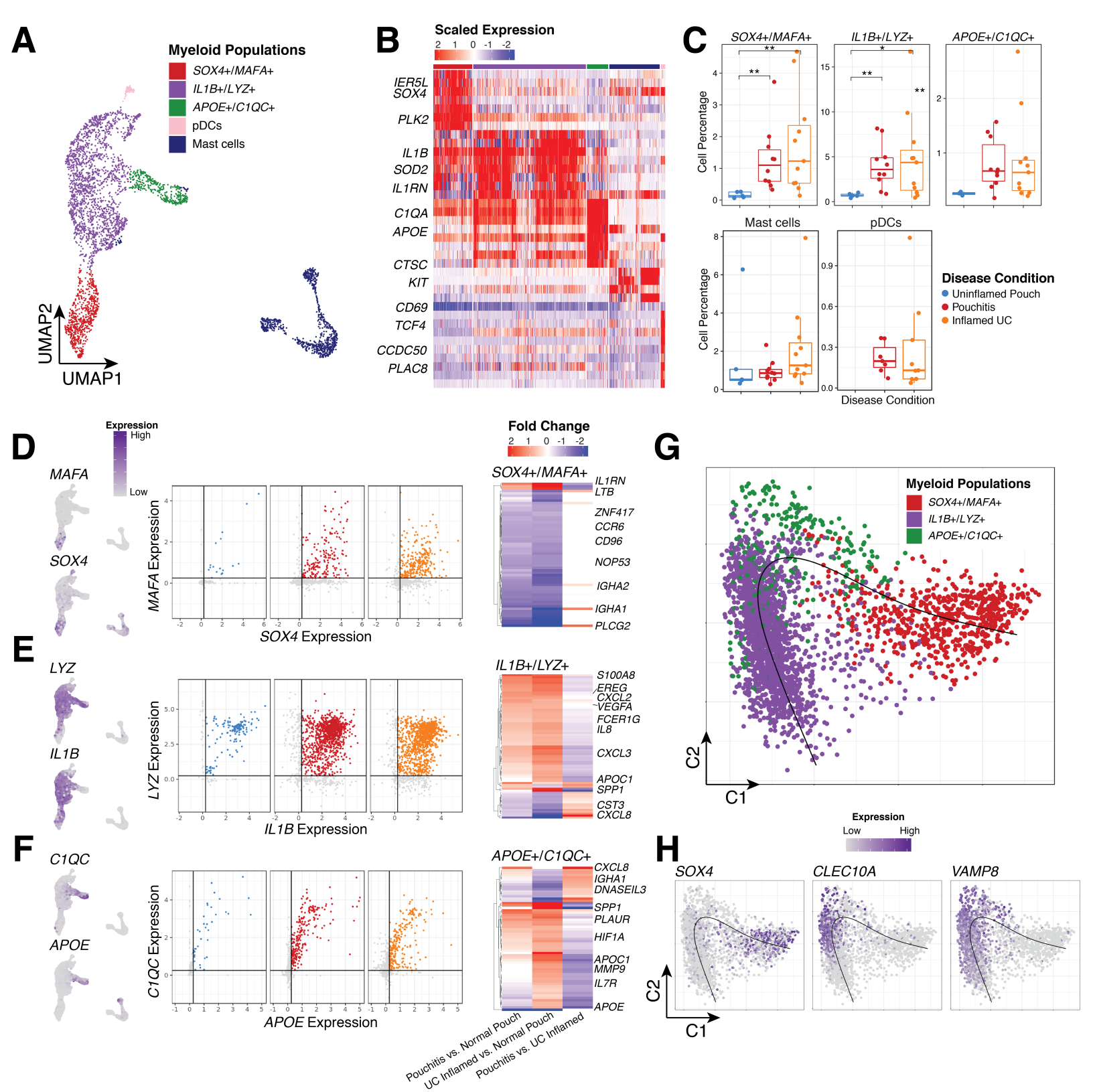
A
Myeloid Populations
SOX4+/MAFA+
IL1B+/LYZ+
APOE+/C1QC+
pDCs
Mast cells
UMAP2
UMAP1
B
Scaled Expression
2 1 0 -1 -2
IER5L
SOX4
PLK2
IL1B
SOD2
IL1RN
C1QA
APOE
CTSC
KIT
CD69
TCF4
CCDC50
PLAC8
C
SOX4+/MAFA+
IL1B+/LYZ+
APOE+/C1QC+
Cell Percentage
Mast cells
pDCs
Disease Condition
Disease Condition
Uninflamed Pouch
Pouchitis
Inflamed UC
D
Expression
High
Low
MAFA
SOX4
MAFA Expression
SOX4 Expression
Fold Change
2 1 0 -1 -2
SOX4+/MAFA+
IL1RN
LTB
ZNF417
CCR6
CD96
NOP53
IGHA2
IGHA1
PLCG2
E
LYZ
IL1B
LYZ Expression
IL1B Expression
IL1B+/LYZ+
S100A8
EREG
CXCL2
VEGFA
FCER1G
IL8
CXCL3
APOC1
SPP1
CST3
CXCL8
F
C1QC
APOE
C1QC Expression
APOE Expression
APOE+/C1QC+
CXCL8
IGHA1
DNASEIL3
SPP1
PLAUR
HIF1A
APOC1
MMP9
IL7R
APOE
Pouchitis vs. Normal Pouch
UC Inflamed vs. Normal Pouch
Pouchitis vs. UC Inflamed
G
Myeloid Populations
SOX4+/MAFA+
IL1B+/LYZ+
APOE+/C1QC+
C2
C1
H
Expression
Low
High
SOX4
CLEC10A
VAMP8
C2
C1

Figure 2. Increased accumulation of myeloid cell populations in inflamed pouchitis and ulcerative colitis patients. (A) Census of myeloid cell types and visualization by UMAP. (B) Heatmap of scaled expression profiles of myeloid clusters, with selected genes of interests shown on left. (C) Boxplots showing cell cluster frequency of the major populations as a percentage of total cells of each patient shown as individual datapoints, compared between patient groups. (D-F) Feature plots showing representative UMAPs of marker gene pairs (left), gene by gene expression plots (center) and differential expression heatmaps of log2 fold change between Uninflamed Pouch, Pouchitis and UC inflamed samples (right) in *SOX4*+/*MAFA*+ (D), *IL1B*+/*LYZ*+ (E) and *APOE*+/*C1QC*+ Monocyte/Macrophage populations. Significantly expressed genes are determined by Log2 fold change greater than 0.75 and adjusted p-value less than 0.05. (G) Diffusion map of *IL1B*+/*LYZ*+, *SOX4*+/*MAFA*+ and *APOE*+/*C1QC*+ monocyte/macrophages (top) with a psuedotime projection (black line). (H) *SOX4*, *CLEC10A* and *VAMP8* normalized expression shown on diffusion map as feature plots (bottom). Asterisks indicate significance testing for Wilcoxon ranked test, * = $p < 0.05$, ** = $p < 0.01$, *** = $p < 0.001$.

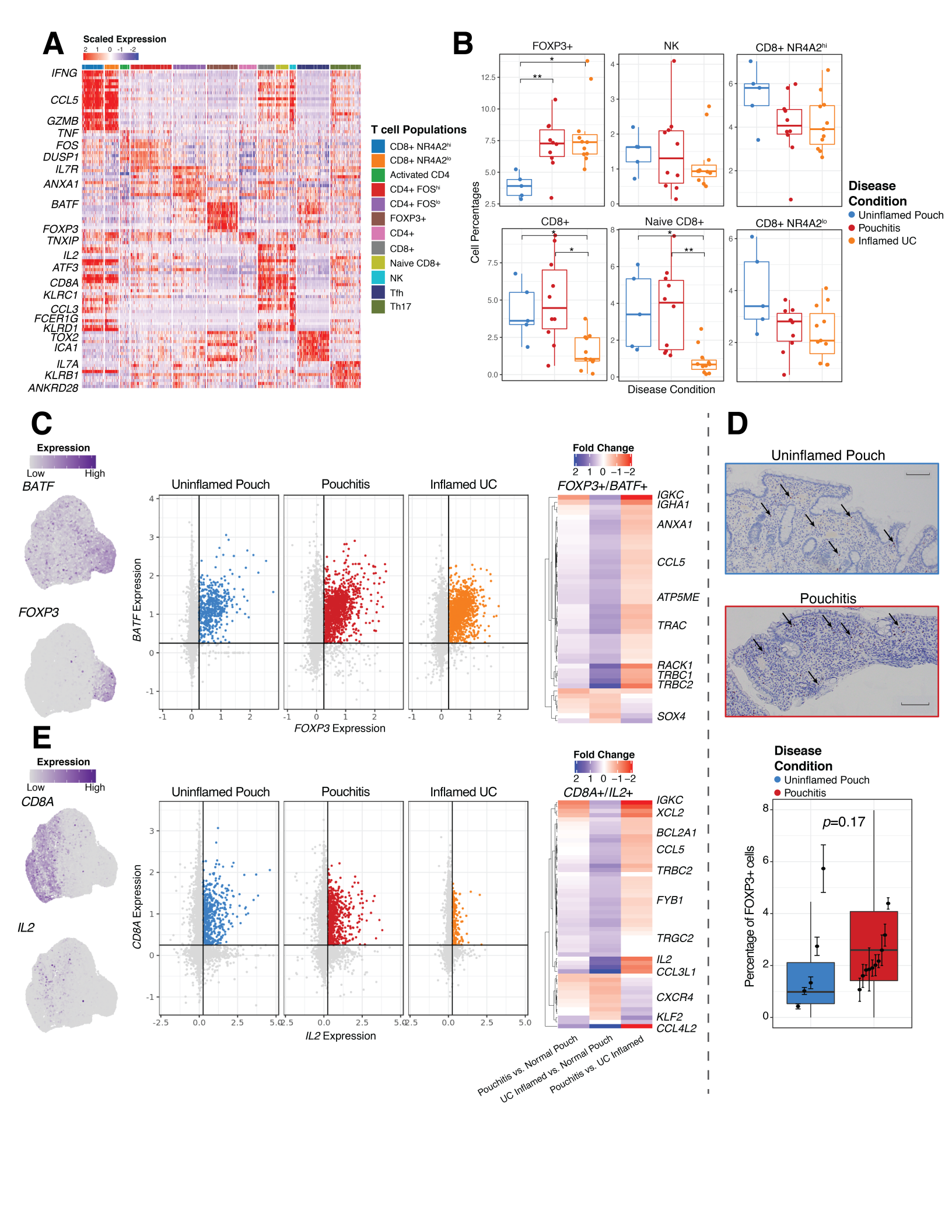
A
Scaled Expression
2 1 0 -1 -2
IFNG
CCL5
GZMB
TNF
FOS
DUSP1
IL7R
ANXA1
BATF
FOXP3
TNXIP
IL2
ATF3
CD8A
KLRC1
CCL3
FCER1G
KLRD1
TOX2
ICA1
IL7A
KLRB1
ANKRD28
T cell Populations
CD8+ NR4A2hi
CD8+ NR4A2lo
Activated CD4
CD4+ FOShi
CD4+ FOSlo
FOXP3+
CD4+
CD8+
Naive CD8+
NK
Tfh
Th17
B
FOXP3+
NK
CD8+ NR4A2hi
CD8+
Naive CD8+
CD8+ NR4A2lo
Cell Percentages
Disease Condition
Disease Condition
Uninflamed Pouch
Pouchitis
Inflamed UC
C
Expression
Low
High
BATF
FOXP3
Uninflamed Pouch
Pouchitis
Inflamed UC
BATF Expression
FOXP3 Expression
Fold Change
2 1 0 −1 −2
FOXP3+/BATF+
IGKC
IGHA1
ANXA1
CCL5
ATP5ME
TRAC
RACK1
TRBC1
TRBC2
SOX4
D
Uninflamed Pouch
Pouchitis
E
Expression
Low
High
CD8A
IL2
Uninflamed Pouch
Pouchitis
Inflamed UC
CD8A Expression
IL2 Expression
Fold Change
2 1 0 −1 −2
CD8A+/IL2+
IGKC
XCL2
BCL2A1
CCL5
TRBC2
FYB1
TRGC2
IL2
CCL3L1
CXCR4
KLF2
CCL4L2
Pouchitis vs. Normal Pouch
UC Inflamed vs. Normal Pouch
Pouchitis vs. UC Inflamed
Disease Condition
Uninflamed Pouch
Pouchitis
p=0.17
Percentage of FOXP3+ cells

Figure 3. Dysregulation of the T cell compartment in inflamed pouchitis and ulcerative colitis patients. (A) Heatmap of scaled expression profiles of the 12 major T cell clusters, with selected genes of interests shown on left. (B) Boxplots showing cell cluster frequency of selected T cell populations as a percentage of total cells of each patient shown as individual datapoints, compared between patient groups. (C) Feature plots showing representative UMAP visualizations of *FOXP3* and *BATF* expression in T cells (left), *FOXP3* by BATF expression plots (center) and differential expression heatmaps of genes with log2 fold change between Uninflamed Pouch, Pouchitis and UC inflamed samples (right) in *FOXP3*+/*BATF*+ T cells. (D) Representative *FOXP3* stained pouch tissue sections (top) and quantification (bottom), where dark brown colored cells indicate *FOXP3* nuclear expression and quantification of percent *FOXP3*+ cells in 5 uninflamed patient samples and 10 pouchitis patient sample. Significance was determined by nested ANOVA correcting for multiple data points per patient. (E) Feature plots showing representative UMAP visualizations of *CD8A* and *IL2* expression in T cells (left), *CD8A* by IL2 expression plots (center) and differential expression heatmaps of log2 fold change between Uninflamed Pouch, Pouchitis and UC inflamed samples (right) in *CD8A*+/*IL2*+ T cells. Selected genes of interests shown on right. Significantly differentially expressed genes are determined by Log2 fold change greater than 0.5 and adjusted p-value less than 0.05. Asterisks indicate significance testing for Wilcoxon ranked test, * = $p < 0.05$, ** = $p < 0.01$, *** = $p < 0.001$. Scale bars indicate 200μm imaged at 10X magnification.

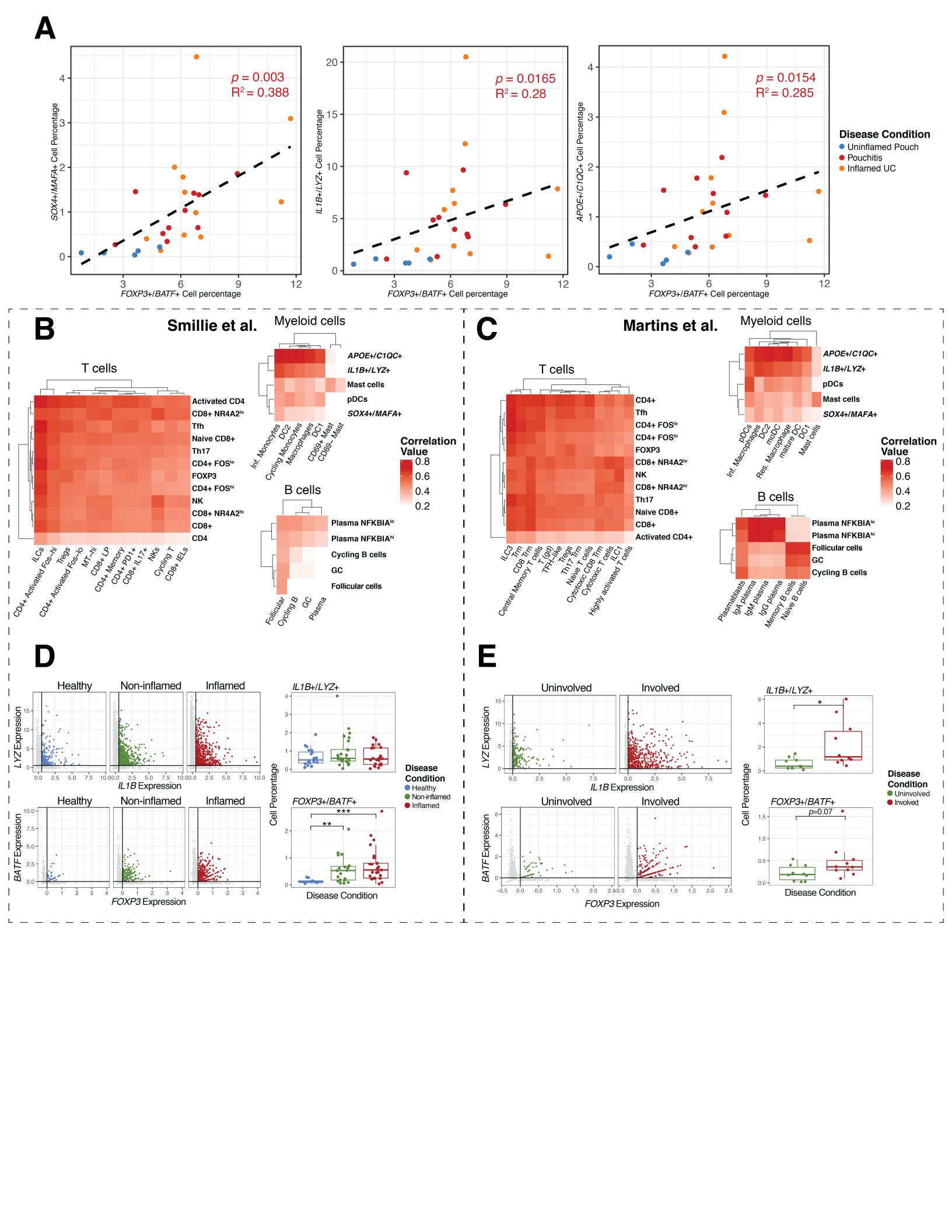
A
p = 0.003
R² = 0.388
SOX4+/MAFA+ Cell Percentage
FOXP3+/BATF+ Cell percentage
p = 0.0165
R² = 0.28
IL1B+/LYZ+ Cell Percentage
FOXP3+/BATF+ Cell percentage
p = 0.0154
R² = 0.285
APOE+/C1QC+ Cell Percentage
FOXP3+/BATF+ Cell percentage
Disease Condition
Uninflamed Pouch
Pouchitis
Inflamed UC
B
Smillie et al.
T cells
Activated CD4
CD8+ NR4A2lo
Tfh
Naive CD8+
Th17
CD4+ FOSlo
FOXP3
CD4+ FOShi
NK
CD8+ NR4A2hi
CD8+
CD4
ILCs
CD4+ Activated Fos–hi
Tregs
CD4+ Activated Fos–lo
MT–hi
CD8+ LP
CD4+ Memory
CD4+ PD1+
CD8+ IL17+
NKs
Cycling T
CD8+ IELs
Myeloid cells
APOE+/C1QC+
IL1B+/LYZ+
Mast cells
pDCs
SOX4+/MAFA+
Inf. Monocytes
DC2
Cycling Monocytes
Macrophages
DC1
CD69+ Mast
CD69– Mast
B cells
Plasma NFKBIAlo
Plasma NFKBIAhi
Cycling B cells
GC
Follicular cells
Follicular
Cycling B
GC
Plasma
Correlation Value
0.8
0.6
0.4
0.2
C
Martins et al.
T cells
CD4+
Tfh
CD4+ FOSlo
CD4+ FOShi
FOXP3
CD8+ NR4A2lo
NK
CD8+ NR4A2hi
Th17
Naive CD8+
CD8+
Activated CD4+
ILC3
Trm
CD8 Trm
Central Memory T cells
T (gd)
TFH–like
Tregs
Th17 Trm
Naive T cells
Cytotoxic CD8 Trm
Cytotoxic T cells
ILC1
Highly activated T cells
Myeloid cells
APOE+/C1QC+
IL1B+/LYZ+
pDCs
Mast cells
SOX4+/MAFA+
pDCs
Inf. Macrophages
DC2
moDC
Res. Macrophage
mature DC
DC1
Mast cells
B cells
Plasma NFKBIAlo
Plasma NFKBIAhi
Follicular cells
GC
Cycling B cells
Plasmablasts
IgA plasma
IgM plasma
IgG plasma
Memory B cells
Naive B cells
Correlation Value
0.8
0.6
0.4
0.2
D
Healthy
Non-inflamed
Inflamed
LYZ Expression
IL1B Expression
BATF Expression
FOXP3 Expression
IL1B+/LYZ+
FOXP3+/BATF+
Cell Percentage
**
***
Disease Condition
Healthy
Non-inflamed
Inflamed
E
Uninvolved
Involved
LYZ Expression
IL1B Expression
BATF Expression
FOXP3 Expression
IL1B+/LYZ+
FOXP3+/BATF+
*
p=0.07
Cell Percentage
Disease Condition
Uninvolved
Involved

Figure 4. Defining cell states related in active inflammation in J-pouch, ulcerative colitis and Crohn's disease. (A) Linear model of the associations between the percentage of *FOXP3*+*BATF*+ cells and *SOX4*+*MAFA*+ (left), *IL1B*+*LYZ*+ (middle) and *APOE*+*C1QC*+ cells (right). R_2 and *p* value was determined by linear regression. Individual samples are shown and color coded based on disease condition. (B, C) Heatmaps of correlated cell types from scRNA-seq datasets of Smillie et al. (B) and Martins et al. (C), comparing T cell (left), myeloid subsets (top) and B cell subsets (bottom). (D) Single cell expression of *IL1B* and *LYZ* (top) and relative percentage of LYZ+IL1B+ cell populations from healthy, inflamed and non-inflamed ulcerative colitis patient samples from Smillie et al. Single cell expression of *FOXP3* and *BATF* (bottom) and relative percentage of *FOXP3*+*BATF*+ cell populations from healthy, inflamed and non-inflamed ulcerative colitis patients samples from Smillie et al. (E) Single cell expression of *IL1B* and *LYZ* (top) and relative percentage of LYZ+IL1B+ cell populations from matched involved and uninvolved Crohns disease patient samples from Martins et al. Single cell expression of *FOXP3* and *BATF* (bottom) and relative percentage of *FOXP3*+*BATF*+ cell populations from involved and uninvolved Crohns disease patient samples from Martins et al. Asterisks indicate significance testing for Wilcoxon ranked test, * = $p < 0.05$, ** = $p < 0.01$, *** = $p < 0.001$.

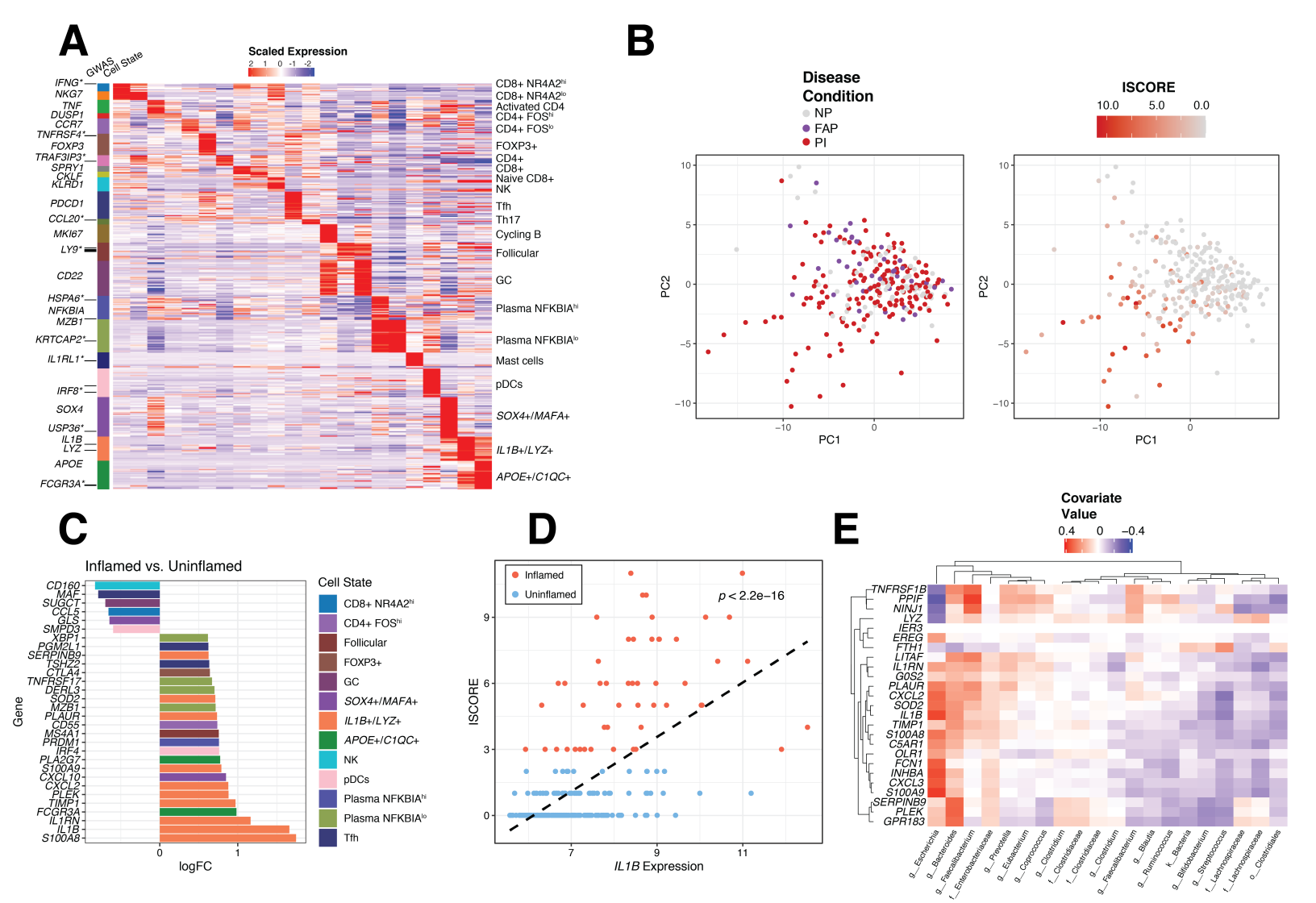
A
Scaled Expression
2 1 0 -1 -2
GWAS
Cell State
IFNG*
NKG7
TNF
DUSP1
CCR7
TNFRSF4*
FOXP3
TRAF3IP3*
SPRY1
CKLF
KLRD1
PDCD1
CCL20*
MKI67
LY9*
CD22
HSPA6*
NFKBIA
MZB1
KRTCAP2*
IL1RL1*
IRF8*
SOX4
USP36*
IL1B
LYZ
APOE
FCGR3A*
CD8+ NR4A2hi
CD8+ NR4A2lo
Activated CD4
CD4+ FOShi
CD4+ FOSlo
FOXP3+
CD4+
CD8+
Naive CD8+
NK
Tfh
Th17
Cycling B
Follicular
GC
Plasma NFKBIAhi
Plasma NFKBIAlo
Mast cells
pDCs
SOX4+/MAFA+
IL1B+/LYZ+
APOE+/C1QC+
B
Disease Condition
NP
FAP
PI
ISCORE
10.0 5.0 0.0
PC1
PC2
C
Inflamed vs. Uninflamed
Gene
logFC
Cell State
CD8+ NR4A2hi
CD4+ FOShi
Follicular
FOXP3+
GC
SOX4+/MAFA+
IL1B+/LYZ+
APOE+/C1QC+
NK
pDCs
Plasma NFKBIAhi
Plasma NFKBIAlo
Tfh
D
Inflamed
Uninflamed
p < 2.2e−16
ISCORE
IL1B Expression
E
Covariate Value
0.4 0 −0.4
TNFRSF1B
PPIF
NINJ1
LYZ
IER3
EREG
FTH1
LITAF
IL1RN
GOS2
PLAUR
CXCL2
SOD2
IL1B
TIMP1
S100A8
C5AR1
OLR1
FCN1
INHBA
CXCL3
S100A9
SERPINB9
PLEK
GPR183
g__Escherichia
g__Bacteroides
g__Faecalibacterium
f__Enterobacteriaceae
g__Prevotella
g__Eubacterium
g__Coprococcus
g__Clostridium
f__Clostridiaceae
f__Clostridiales
g__Clostridium
g__Faecalibacterium
g__Blautia
g__Ruminococcus
k__Bacteria
g__Bifidobacterium
g__Streptococcus
f__Lachnospiraceae
f__Lachnospiraceae
o__Clostridiales

Figure 5. Identification of immune cell type specific transcripts and analysis of an independent dataset of patients with IPAA. (A) Heatmap illustration of a signature matrix of 453 marker genes for 22 identifiable T, B and Myeloid cell states from scRNA-seq. Asterisks indicate GWAS genes related to inflammatory bowel disease and the expression of these genes in the specific cell types on the right. (B) Principal component analysis of 250 IPAA patient samples with familial adenomatous polyposis (FAP), active pouchitis (PI) or no pouchitis (NP) based on the 453-gene signature and colored by Disease Condition (left) and inflammation score (ISCORE) (right). (C) Expression of *IL-1B+/LYZ+* monocyte/macrophage cell type specific transcripts from biopsy samples collected from inflamed (ISCORE > 2) versus uninflamed (ISCORE < 2) patient samples. Shown are log fold change values of the most differentially expressed genes from the 453 cell type specific markers colored by the corresponding cell type from scRNA-seq. (D) Linear model of the association between IL1B expression and the numeric inflammation score for 250 patient samples of IPAA. (E) sPLS analysis of a 25-gene signature for *IL-1B+/LYZ+* monocyte/macrophages compared to microbial taxa measured by 16S rRNA sequencing of the 250 patient samples of IPAA. Directionality of the association between gene expression and bacterial abundance is colored in red or blue as shown in the legend.

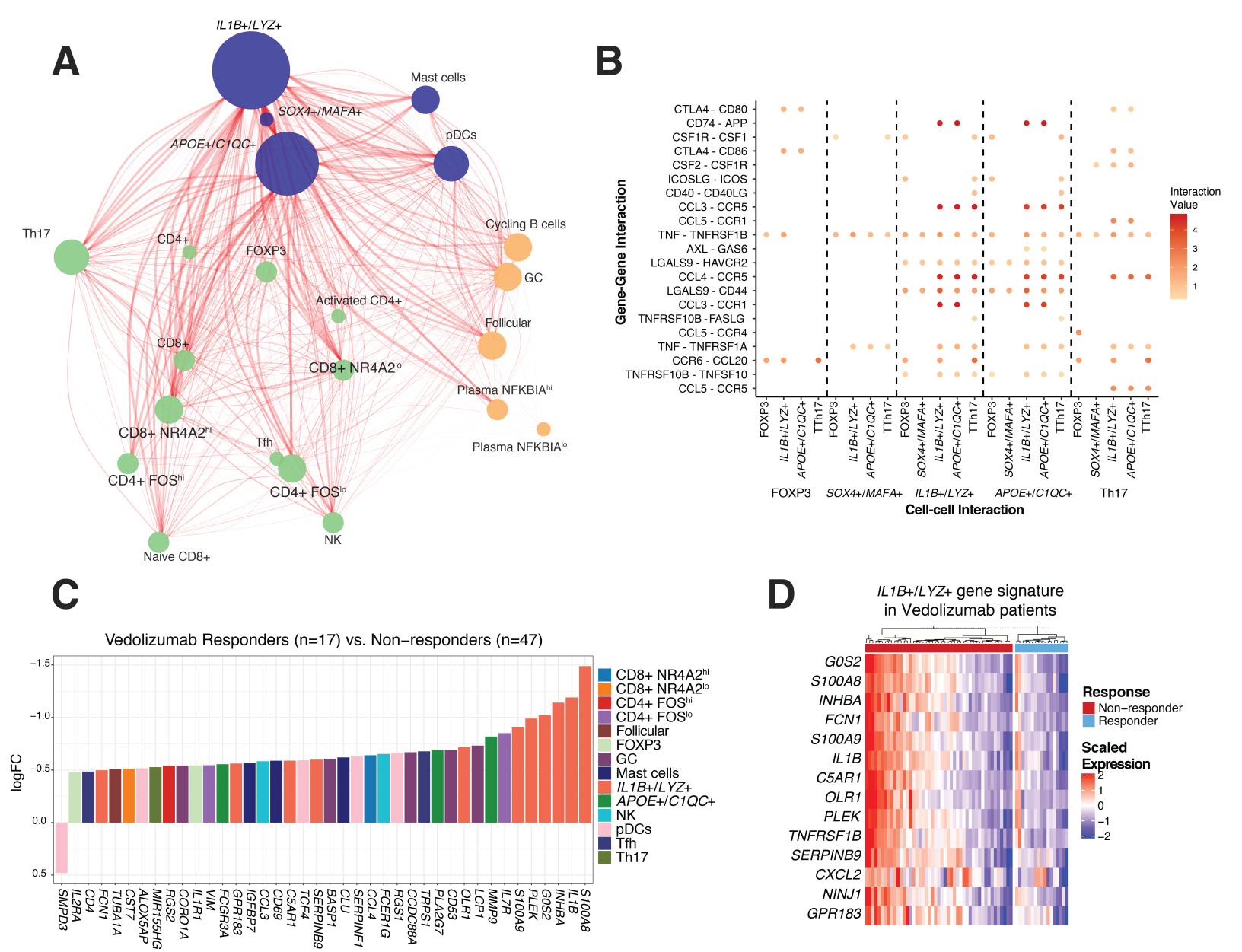
A
IL1B+/LYZ+
Mast cells
SOX4+/MAFA+
pDCs
APOE+/C1QC+
Th17
CD4+
FOXP3
Cycling B cells
GC
Activated CD4+
Follicular
CD8+
CD8+ NR4A2lo
Plasma NFKBIAhi
CD8+ NR4A2hi
Tfh
Plasma NFKBIAlo
CD4+ FOShi
CD4+ FOSlo
NK
Naive CD8+
B
CTLA4 - CD80
CD74 - APP
CSF1R - CSF1
CTLA4 - CD86
CSF2 - CSF1R
ICOSLG - ICOS
CD40 - CD40LG
CCL3 - CCR5
CCL5 - CCR1
TNF - TNFRSF1B
AXL - GAS6
LGALS9 - HAVCR2
CCL4 - CCR5
LGALS9 - CD44
CCL3 - CCR1
TNFRSF10B - FASLG
CCL5 - CCR4
TNF - TNFRSF1A
CCR6 - CCL20
TNFRSF10B - TNFSF10
CCL5 - CCR5
Gene-Gene Interaction
Interaction Value
FOXP3
IL1B+/LYZ+
APOE+/C1QC+
TTh17
SOX4+/MAFA+
Cell-cell Interaction
C
Vedolizumab Responders (n=17) vs. Non−responders (n=47)
logFC
SMPD3
IL2RA
CD4
FCN1
TUBA1A
CST7
ALOX5AP
MIR155HG
RGS2
CORO1A
IL1R1
VIM
FCGR3A
GPR183
IGFBP7
CCL3
CD69
C5AR1
TCF4
SERPINB9
BASP1
CLU
SERPINF1
CCL4
FCER1G
RGS1
CCDC88A
TRPS1
PLA2G7
CD53
OLR1
LCP1
MMP9
IL7R
S100A9
PLEK
G0S2
INHBA
IL1B
S100A8
CD8+ NR4A2hi
CD8+ NR4A2lo
CD4+ FOShi
CD4+ FOSlo
Follicular
FOXP3
GC
Mast cells
IL1B+/LYZ+
APOE+/C1QC+
NK
pDCs
Tfh
Th17
D
IL1B+/LYZ+ gene signature
in Vedolizumab patients
G0S2
S100A8
INHBA
FCN1
S100A9
IL1B
C5AR1
OLR1
PLEK
TNFRSF1B
SERPINB9
CXCL2
NINJ1
GPR183
Response
Non−responder
Responder
Scaled Expression

Figure 6. Evaluating response to clinical therapies and inflammation status in ulcerative colitis. (A) Analysis of receptor-ligand network connections between 22 of the major cell populations identified in scRNA-seq. Each node represents a cell population and each edge a significant receptor-ligand association according to curated database, cellPhoneDB. The size of each node is proportional to the number of connected edges and the thickness of the edges is proportional to the significance value of the connection. (B) Visualization of selected ligand–receptor interactions that are specifically enriched between FOXP3+ Tregs, *SOX4+/MAFA+*, *IL1B+/LYZ+*, *APOE+/C1QC+* monocyte/macrophages and Th17 cells. Interaction values are indicated by intensity, scale on right. (C) Expression of *IL-1B+/LYZ+* monocyte/macrophage cell type specific transcripts from biopsy samples collected from ulcerative colitis patient Responders versus Non-responders to treatment with the anti-α4β7 integrin antibody Vedolizumab. Log fold change values of the most differentially expressed genes from a matrix of 453 cell-type specific markers between Responders and Non-responders to treatment are shown. D) Heatmap showing the heterogeneity in the expression of *IL-1B+/LYZ+* monocyte/macrophage cell type specific transcripts among Non-responders to Vedolizumab treatment. Normalized expression values shown for individual patients from Responders (n=17) and Non-responders (n=47).